ACS Catalysis

Research Article

pubs.acs.org/acscatalysis

Nanosheet-Enhanced Rhodium(III)-Catalysis in C−H Activation

Hui Liu, Zhe An, and Jing He*

State Key Laboratory of Chemical Resource Engineering, Beijing University of Chemical Technology, Beijing 100029, China

Supporting Information

ABSTRACT: Rhodium(III)-catalyzed C−H activation has been promoted impressively with ligand-attached nanosheets of layered double hydroxides (LDHs), a natural and/or synthetic anionic layered compound. A yield of >99% and a regioisomeric ratio of >20:1 have been produced in the coupling of alkenes with *N*-(pivaloyloxy)benzamide. The nanosheets have been revealed to enhance the catalytic activity by affording the desired basicity and improve the regioselectivity by serving as the rigid substitution of α-amino acid ligands.

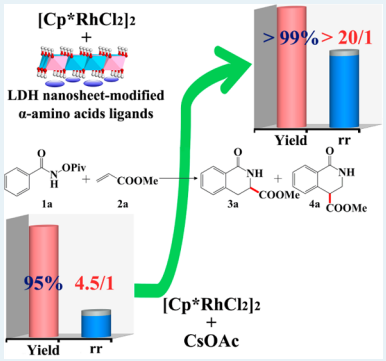

KEYWORDS: *inorganic nanosheet, C−H activation, rigid substitution, rhodium(III) catalyst, solid bases*

INTRODUCTION

Since its first application as a C−H activation catalyst in 2000,[1] the rhodium(III) complex has been attracting increasing attention, because of its lower loading (1−5 mol %) and higher substrates tolerance than the palladium complex, the most early reported and widely used catalyst in C−H activations.[2−8] The rhodium(III) complex was proposed to first activate the ortho-C(sp^2)-H bonds via base-assisted concerted metalation-deprotonation mechanism.[6a,9] To initiate the metalation-deprotonation reaction, the use of a base is indispensable,[2−12] not only for rhodium-catalyzed C−H activations, but also for palladium- and ruthenium-catalyzed C−H activations.[13,14] Generally, $Cu(OAc)_2$, CsOAc, and K_2CO_3, etc. have been employed[9−14] as exogenous solution bases. The use of solid bases, which are much more environment-friendly and green, has not been reported so far in the C−H activations.

The base-assisted activation of ortho-C(sp^2)-H bonds generated a rhodacycle intermediate, which was regioselectively accessed by the attacking substrates (the other alkenes/alkynes).[5f,6a,9] A regioisomeric ratio of 4.5:1 was produced in the regioselective coupling reaction of methyl acrylate with *N*-(pivaloyloxy) benzamide.[6a] Increasing the steric hindrance around Rh center could enhance the regioisometric ratio. For example, anchoring a biotinylated $RhCp^{biotin}(OAc)_2$ complex in the active site of the streptavidin tetramer, which has a pocket geometry to direct the access trajectory of the attacking alkenes to the C−Rh bond, promoted the regioisomeric ratio to 19:1.[15] Elaborately designed strategies, which are simple but could effectively improve regioisomeric selectivity, are highly desired.

Here, we propose an efficient strategy to promote rhodium-(III)-catalyzed C−H activations (Scheme 1), which simply utilizes inorganic nanosheets to modify α-amino acid ligands. α-Amino acids, which are well-known and naturally occurring ligands for metal-catalyzed reaction,[16] have not been employed as ligands in Rh-catalyzed C−H activation reaction. In the Rh(III)-catalyzed C−H activation reaction, only if the nanosheets bearing α-amino acid anions could supply the desired basicity for the activation of base-assisted ortho-C(sp^2)-H bond of *N*-(pivaloyloxy)benzamide (**1a**, for example), the reaction might be initiated. In the regioselective access of the attacking alkene (**2a**, for example) to the rhodacycle intermediate, only if the nanosheets could provide the desired steric hindrance around a Rh(III) center, a highly regioselective product might then be produced. The inorganic nanosheets employed here are the positively charged brucite-like layers of layered double hydroxides (LDHs), a natural and/or synthetic anionic compound and also well-known basic catalysts.[17] The strategy proposed here demonstrates impressive efficacy, in that >99% yield and >20:1 regioisomeric ratio have been obtained in the coupling reaction of alkenes with *N*-(pivaloyloxy)benzamide catalyzed by the rhodium(III) centers with LDH nanosheet modified α-amino acid anions as ligands.

EXPERIMENTAL SECTION

Chemicals. Methyl acrylate, ethyl acrylate, *n*-butyl acrylate, phenyl acrylate, styrene, 4-methoxystyrene, 4-chlorostyrene, 4-nitrostyrene, 1-hexene, *tert*-butyl hydroxycarbamate, pivalic anhydride, triflic acid, benzohydroxamic acid, 4-methoxybenzoyl chloride, 4-chlorobenzoyl chloride, 4-fluorobenzoyl chloride, 4-nitrobenzoyl chloride, and $[Cp^*RhCl_2]_2$ were purchased from Sigma−Aldrich and Alfa Aesar. All the reagents

Received: April 25, 2014
Revised: August 22, 2014
Published: September 3, 2014

   dx.doi.org/10.1021/cs500558s | ACS Catal. 2014, 4, 3543−3550

Scheme 1. Schematic Illustration of Designed Rh(III) Catalysts with (A) LDH Nanosheets-Modified α-Amino Acid Anions as Ligands, (B) the Cp* Ligand Positioned Parallel to the LDH Nanosheet, (C) Activation of the C−H Bonds of *N*-(pivaloyloxy)benzamide by Rh(III) Center with the Assistance of LDH Nanosheets, and (D) Regioselective Access of Attacking Alkenes to the C−Rh Bond[a]

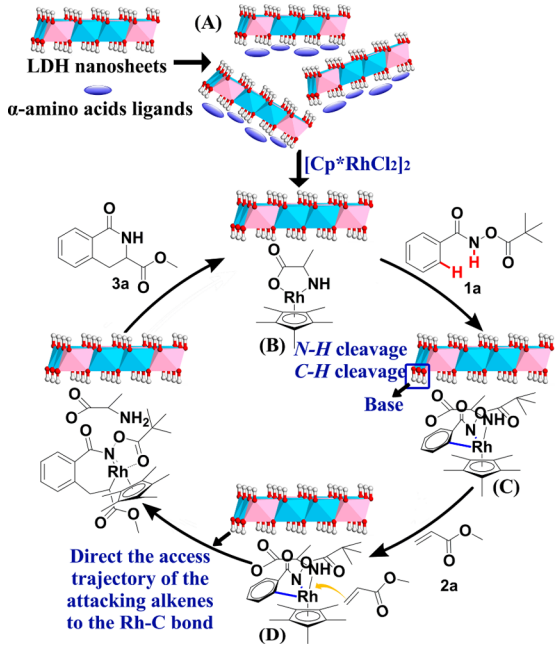

[a]The α-amino acid anions employed here include L-alanine, L-serine, L-leucine, L-histidine, and L-proline.

and commercial chemicals were of analytical purity and used as received without further purification. The catalyzed substrates *N*-(pivaloyloxy)benzamide (**1a**), 4-methoxyl-*N*-(pivaloyloxy)-benzamide (**1e**), 4-chloro-*N*-(pivaloyloxy)benzamide (**1f**), 4-fluoro-*N*-(pivaloyloxy)benzamide (**1g**), and 4-nitro-*N*-(pivaloyloxy)benzamide (**1h**) were synthesized following the procedure reported previously.[6a]

Synthesis of *N*-(pivaloyloxy)benzamide. Pivalic anhydride (18.3 mmol, 3.70 mL, 1 equiv) was added to a suspension of benzohydroxamic acid (21.9 mmol, 3.0 g, 1.2 equiv) in dichloromethane (100 mL). The resulting mixture was allowed to stir at room temperature for 16 h. It was then transferred to a separatory funnel and washed with saturated $NaHCO_3$. The organic phase was dried over $MgSO_4$, filtered, and evaporated under reduced pressure. The purification was made by flash column chromatography using 15% EtOAc in hexane as eluent. The product obtained is a white solid. The structure was confirmed by comparison with ^1H NMR data shown in the literature.[6a]

General Procedure for the Synthesis of Pivaloyl Protected Hydroxamic Acid Derivatives. To a solution of 2 parts EtOAc (24 mL) in one part H_2O (12 mL) containing Na_2CO_3 (424 mg, 4.0 mmol, 2 equiv) was added *O*-pivaloylhydroxyamine triflic acid (534 mg, 2 mmol, 1 equiv).[6a] The mixture was cooled to 0 °C and *para*-substituted benzoyl chloride (2 mmol, 2 equiv) was added to the mixture. It was then allowed to stir at 0 °C for 2 h. The reaction was then quenched with saturated $NaHCO_3$ and more EtOAc were added. The organic phase was washed twice with saturated $NaHCO_3$. It was then dried over $MgSO_4$, filtered, and evaporated under reduced pressure. The purification was made by flash column chromatography using 25% EtOAc in hexane as the eluent. The product obtained is a white solid. The structures were determined by nuclear magnetic resonance (^1H NMR and ^{13}C NMR), Fourier transform infrared (FT-IR) spectroscopy, and high-resolution mass spectroscopy (HRMS).

Preparation and Delamination of LDH Nanosheets-Modified α-Amino Acid (AA) Anions. The preparation of M^{II}/Al-AA-LDHs (AA = L-alanine, L-serine, L-leucine, and L-histidine) were accomplished through the co-precipitation approach[18] by addition of a mixed solution of 1 M $M(NO_3)_2$ (M = Mg, Ni, Zn) and $Al(NO_3)_3$ (or 1 M MCl_2 (M = Mg, Ni, and Zn) and $AlCl_3$) dropwise to a stirred 50 mM α-amino acid solution (M^{2+}/Al^{3+}/α-amino acid molar ratio = 2/1/1). The solution pH was maintained at 10 for Mg/Al-AA-LDHs, 8 for Ni/Al-AA-LDHs, and 9 for Zn/Al-AA-LDHs by dropwise addition of 1 M NaOH solution under stirring. The suspension was stirred at 313 K in N_2 atmosphere for 6 h. The resulting suspension was filtrated, washed with decarbonated deionized water and anhydrous alcohol, and dried in a vacuum oven at room temperature. The preparation of Mg/Al-Pro-LDHs was accomplished through a reconstruction method.[19] The Mg/Al-CO_3^{2-}-LDHs precursor was synthesized by the addition of a mixed solution of 0.16 M $Mg(NO_3)_2$ and $Al(NO_3)_3$ (Mg/Al molar ratio = 3/1) in 225 mL of deionized water to a stirred solution of NaOH and Na_2CO_3 in 225 mL of deionized water with pH maintained at 9.5. The concentrations of the base were related to the concentrations of metal ions: $[NaOH] = 1.6[Mg^{2+} + Al^{3+}]$ and $[CO_3^{2-}] = 2.0[Al^{3+}]$. The suspension was aged at 373 K for 18 h. The final precipitate was filtered, washed with deionized water, and dried at 333 K for 24 h. The Mg/Al-CO_3^{2-}-LDHs was calcined at 773 K for 5 h with a temperature-programmed rate of 5 K/min from room temperature to 773 K, and then naturally cooled, producing LDO. Then, 0.5 g of LDO was added to a freshly prepared solution of 0.756 g of L-proline and 0.24 g of NaOH in 100 mL of decarbonated deionized water. The suspension was stirred at 298 K in N_2 atmosphere for 24 h. The resulting precipitate was filtered, washed with deionized and decarbonated water twice and anhydrous ethanol, and dried in a vacuum oven at 313 K.

The delamination of α-amino acid intercalated LDHs was achieved through the abundant use of water, following the procedure reported previously[20] with some modification. Typically, α-amino acid intercalated LDH solid was suspended in 30 mL of decarbonated deionized water in a conical beaker, which was sealed airtight after purging with N_2 gas for 0.5 h. Then, the suspension was treated by ultrasonic treatment at 0 °C until the suspension appeared transparent.

Basicity Measurements. The basicities of the α-amino acids modified LDHs were evaluated by the indicator titration method.[21] The color of the indicators adsorbed on the solid was visually observed after the addition of 5 mL of purified benzene and one drop of a certain indicator solution to 0.1 g of LDHs solid in a 25 mL conical flask. The indicators used are phenolphthalein (pK_{BH} = 9.6), 2,4,6-trinitroaniline (pK_{BH} = 12.2), 2,4-dinitroaniline (pK_{BH} = 15.0), and 4-chloro-2-nitroaniline (pK_{BH} = 17.2).

Characterization. ^1H and ^{13}C NMR spectra were recorded in $CDCl_3$ or DMSO-d_6 solutions on Bruker Avance 400 MHz NMR spectrometer (Bruker, Bremen, Germany) at ambient temperature. ^1H NMR data are reported as the following: chemical shift in parts per million (δ, ppm) from chloroform ($CHCl_3$) taken as 7.26 ppm, intergration, multiplicity (s =

dx.doi.org/10.1021/cs500558s | ACS Catal. 2014, 4, 3543−3550

singlet, d = doublet, t = triplet, q = quartet, m = multiplet, dd = doublet of doublets) and coupling constant (Hz). ^{13}C NMR data are reported as the following: chemical shifts are reported in ppm from $CDCl_3$ taken as 77.0 ppm. The powder X-ray diffraction (XRD) patterns were taken on a Shimadzu Model XRD-6000 diffractometer with Cu Kα radiation (40 kV and 30 mA) at a scanning rate of 5°/min and step size of 0.02°. The content of Mg, Ni, Zn, Rh, and Al was determined on inductively coupled plasma (ICP) atomic emission spectrophotometry (Shimadzu, Model ICPs-7500) by dissolving the samples in dilute HNO_3. The C, H and N element analysis was performed on an Elementar Co. Vario elemental analyzer. The Fourier transform infrared (FT-IR) spectra were recorded on a Bruker Vector 22 FT-IR spectrometer with a resolution of 4 cm^{-1} using the standard KBr pellet method. The XPS measurements were carried out using an ESCALAB Model 250Xi spectrometer. A monochromatized aluminum source (Al Kα = 1486.6 eV) was used for excitation.

General Procedure for the C−H Activation Reactions. Without any particular precautions to extrude oxygen or moisture, the delaminated M^{II}/Al-AA-LDHs (AA: 0.55 mmol %, water: 1.75 mL), $[Cp^*RhCl_2]_2$ (0.5 mol %) in MeOH (0.2 M) were weighed in a flask and subjected to stirring for 10 min. The pivaloyl protected hydroxamic acid (1 equiv, 33 mg, 0.15 mmol) and the alkene (1.2 equiv) was then added and the reaction was sealed and subjected to stirring at 25 °C. After 12 h, the reaction was quenched with 5 mL of *n*-hexane/ethyl acetate (v/v = 5/1) and the water phase was washed twice with *n*-hexane/ethyl acetate (v/v = 5/1). The organic phase was then dried over Na_2SO_4, filtered and evaporated under reduced pressure. Internal standard 1,3,5-triisopropylbenzene (1 equiv) was added into the crude product. The conversion, yield, and regioselectivity were determined by ^{1}H NMR.

Catalyst Recycling. The catalyst recycling was simply achieved by liquid/liquid separation. The reaction product and unreacted starting reagents were removed from the aqueous reaction mixture by extraction with 5 mL of *n*-hexane/ethyl acetate (v/v = 5/1) three times after the reaction terminated. 745 μL of MeOH, fresh *N*-(pivaloyloxy)benzamides, and methyl acrylate were added into the aqueous solution for the next reaction. As for the reaction system with Mg/Al-CO_3^{2-}-LDHs as the base, the solid was recovered by filtration after the reaction terminated and washed with 5 mL of *n*-hexane/ethyl acetate (v/v = 5/1) three times. The liquid mixture was extracted with 5 mL of *n*-hexane/ethyl acetate (v/v = 5/1) three times. The aqueous solution was used for the next run.

RESULTS AND DISCUSSION

Structural Properties of LDH Nanosheets-Modified α-Amino Acid Anions. The magnesium and aluminum hydroxides (Mg/Al-LDHs), with the strongest basicity,[17b−e] are first employed as hosts in this work. The intercalation of L-alanine (Ala), L-serine (Ser), L-leucine (Leu), and L-histidine (His) was performed by the co-precipitation and of L-proline (Pro) by the reconstruction method. The corresponding 003 reflections in the XRD patterns at 2θ = 11.1°, 10.9°, 10.8°, 10.7°, and 11.3° give basal spacings of 0.80, 0.81, 0.82, 0.83, and 0.78 nm (see Figure 1A). Subtracting the brucite-like layer thickness (0.48 nm), the interlayer spacing is estimated to be 0.32, 0.33, 0.34, 0.35, and 0.30 nm, indicating a monolayer horizontal arrangement of interlayer amino acid (AA) anions in light of the dimensions of AA anions measured by Materials Studio Program (0.50 nm × 0.54 nm × 0.30 nm for L-alanine,

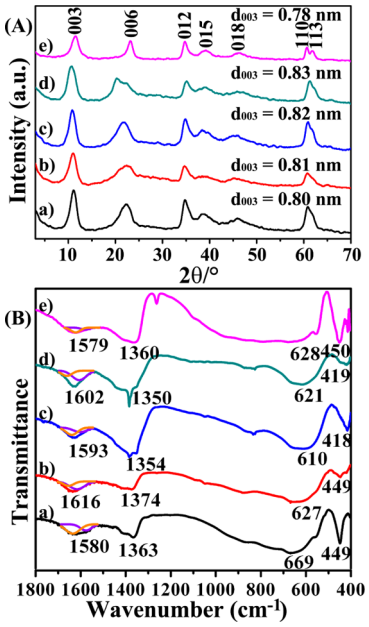

Figure 1. (A) XRD patterns and (B) FT-IR spectra of Mg/Al-Ala-LDHs (spectrum a), Mg/Al-Ser-LDHs (spectrum b), Mg/Al-leu-LDHs (spectrum c), Mg/Al-His-LDHs (spectrum d), and (spectrum e) Mg/Al-Pro-LDHs.

0.65 nm × 0.54 nm × 0.30 nm for L-serine, 0.76 nm × 0.55 nm × 0.30 nm for L-leucine, 0.89 nm × 0.56 nm × 0.31 nm for L-histidine, and 0.64 nm × 0.48 nm × 0.30 nm for L-proline). The asymmetric and symmetric vibrations of carboxylate group in the Mg/Al-LDH nanosheets-attached AA anions are resolved at 1580 and 1363, 1616 and 1374, 1593 and 1354, 1602 and 1350, and 1579 and 1360 cm^{-1} in the FT-IR spectra (Figure 1B). The $\Delta\upsilon_{COO}$ ($\Delta\upsilon_{COO} = \Delta\upsilon_{as} - \Delta\upsilon_{s}$) value is 217, 242, 239, 252, and 219 cm^{-1}, respectively, all of which are larger than the $\Delta\upsilon_{COO}$ value for the corresponding AA sodium salt ($\Delta\upsilon_{COO}$ = 213, 207, 175, 181, and 196 cm^{-1}), revealing a monodentate electrostatic interaction between the carboxylate and the brucite-like layer, according to the previous report.[22]

Then Ni/Al-LDHs and Zn/Al-LDHs are employed as hosts. The corresponding 003 reflections in the XRD patterns at 2θ = 10.9° and 10.4° give the basal spacing of 0.81 and 0.86 nm for the intercalation of L-alanine and at 2θ = 6.10° and 6.20° give the basal spacing of 1.45 and 1.42 nm for the intercalation of L-leucine (Figure 2A). The interlayer spacing is 0.33 nm for Ni/Al-Ala-LDHs, 0.38 nm for Zn/Al-Ala-LDHs, 0.97 nm for Ni/Al-Leu-LDHs, and 0.94 nm for Zn/Al-Leu-LDHs, indicating a monolayer horizontal arrangement of interlayer L-alanine anions for Ni/Al-Ala-LDHs, a monolayer tilted arrangement for Zn/Al-Ala-LDHs, and a monolayer vertical arrangement of interlayer L-leucine anions for Ni/Al-Leu-LDHs and Zn/Al-Leu-LDHs. The asymmetric and symmetric vibrations of carboxylate group in the LDH nanosheets-attached AA are resolved at 1616 and 1370, 1603 and 1355, 1576 and 1353, and 1599 and 1364 cm^{-1} in the FT-IR spectra (Figure 2B). The $\Delta\upsilon_{COO}$ is 246, 248, 223, and 235 cm^{-1}, revealing monodentate interaction. The chemical compositions for the M^{II}/Al-AA-LDHs solids were determined as $[Mg_{0.77}Al_{0.23}(OH)_2](Ala)_{0.11}(CO_3)_{0.02}Cl_{0.08}\cdot 0.29\ H_2O$, $[Mg_{0.74}Al_{0.26}(OH)_2](Ser)_{0.08}(CO_3)_{0.03}Cl_{0.12}\cdot 0.62\ H_2O$, $[Mg_{0.78}Al_{0.22}(OH)_2](Leu)_{0.05}(NO_3)_{0.17}\cdot 0.31\ H_2O$, $[Mg_{0.78}Al_{0.22}(OH)_2](His)_{0.04}(NO_3)_{0.18}\cdot 0.19\ H_2O$, $[Mg_{0.76}Al_{0.24}(OH)_2](Pro)_{0.04}$

dx.doi.org/10.1021/cs500558s | ACS Catal. 2014, 4, 3543−3550

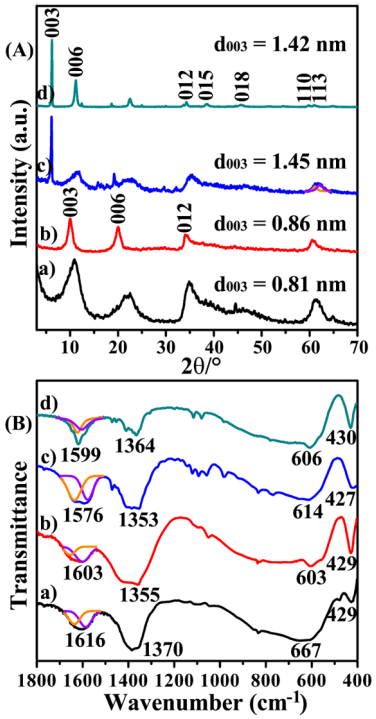

Figure 2. (A) XRD patterns and (B) FT-IR spectra of Ni/Al-Ala-LDHs (spectrum a), Zn/Al-Ala-LDHs (spectrum b), Ni/Al-Leu-LDHs (spectrum c), and Zn/Al-Leu-LDHs (spectrum d).

$(CO_3)_{0.10}\cdot 0.53\ H_2O$, $[Ni_{0.73}Al_{0.27}(OH)_2]\ (Ala)_{0.10}(NO_3)_{0.17}\cdot 0.61\ H_2O$, $[Zn_{0.77}Al_{0.23}(OH)_2](Ala)_{0.09}(NO_3)_{0.14}\cdot 0.25\ H_2O$, $[Ni_{0.74}Al_{0.26}(OH)_2]\ (Leu)_{0.17}(NO_3)_{0.09}\cdot 0.27\ H_2O$, $[Zn_{0.75}Al_{0.25}(OH)_2](Leu)_{0.09}(CO_3)_{0.02}Cl_{0.12}\cdot 0.17\ H_2O$ based on the ICP and CHN analysis results. The LDHs intercalated with AA anions are delaminated in water to colloid in prior to use as the C−H activation catalyst.

Application of LDH Nanosheets-Modified α-Amino Acid Anions in Rh-Catalyzed C−H Activation Reaction. The delaminated M^{II}/Al-AA-LDHs were applied together with $[Cp^*RhCl_2]_2$ in the C−H activation reaction of *N*-(pivaloyloxy)benzamide (**1a**) with methyl acrylate (**2a**) in MeOH/H_2O medium at 25 °C. Inspiringly, >99% conversion of **1a** and >99% yield of dihydroisoquinolone were obtained in 12 h for delaminated Mg/Al-Ala-LDHs (Table 1, entry 1). The isolated yield (95%) is consistent with the ^{1}H NMR yield. Conversions of >99%, 97%, 98%, and >99% and yields of 96%, 96%, 96%, and 97% were produced for delaminated Mg/Al-Ser-LDHs, Mg/Al-Leu-LDHs, Mg/Al-His-LDHs, and Mg/Al-Pro-LDHs (Table 1, entries 2−5). With an attempt to obtain asymmetric induction in the product by using single chiral AA ligands, only delaminated Mg/Al-Ala-Cp*Rh-LDHs provide 7% ee. (The ee of racemic product is 2%.) This is supposed to result from a smaller dimension of L-alanine among all the AA, which provides a closer distance between its chiral center and the nanosheet, so that the nanosheet is able to serve as a rigid substituent[23] to facilitate the asymmetric induction of L-alanine. The C−H activation occurred in the absence of exogenous solution bases, indicating that the desired basicity for C−H activation originated from LDH nanosheets, just as expected. Without Mg/Al-AA-LDHs, none of the desired product was observed (Table 1, entry 6). Only a trace amount of product was afforded by L-histidine and its corresponding sodium salt, with the strongest basicity in the AA employed in this work (Table 1, entries 7 and 8). The experiment with other four AA and their sodium salts as an exogenous base was also examined, and only a trace amount of product was afforded. Using K_2CO_3, which could not provide the desired basicity, only a trace amount of product was observed (Table 1, entry 9). Even within 24 h, 83% conversion and 67% yield were achieved, using CsOAc as exogenous solution base (Table 1, entry 10). The higher activity of Mg/Al-AA-LDHs than CsOAc is supposed to result from two reasons. First, the delamination of nanosheets allows the catalytic C−H activation reactions to be carried out under pseudo-homogeneous reaction conditions. The solid/liquid interfacial diffusion limitation is greatly

Table 1. Effects of LDH Nanosheets on Rh-Catalyzed C−H Activation Reaction of *N*-(pivaloyloxy)benzamide with Methyl Acrylate[a]

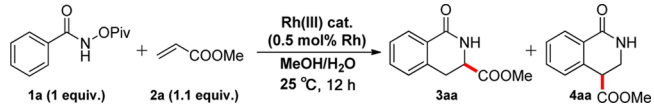

entry	catalyst	base	conversion of **1a**[b] (%)	yield of **3a**[b] (%)	regioisomeric ratio[b]
1	delaminated Mg/Al-Ala-Cp*Rh-LDHs		>99 (>99)	>99 (>99)[c]	>20:1 (>20:1)
2	delaminated Mg/Al-Ser-Cp*Rh-LDHs		>99 (98)	96 (96)	>20:1 (>20:1)
3	delaminated Mg/Al-Leu-Cp*Rh-LDHs		97 (98)	96 (96)	>20:1 (>20:1)
4	delaminated Mg/Al-His-Cp*Rh-LDHs		98 (94)	96 (93)	>20:1 (>20:1)
5	delaminated Mg/Al-Pro-Cp*Rh-LDHs		>99 (98)	97 (96)	>20:1 (>20:1)
6	$[Cp^*RhCl_2]_2$		<5 (<5)	trace (trace)	nd[d] (nd)
7	$[Cp^*RhCl_2]_2$	L-His	<5	trace	nd[d]
8	$[Cp^*RhCl_2]_2$	HisNa	<5	trace	nd[d]
9	$[Cp^*RhCl_2]_2$	K_2CO_3	<5 (<5)	<5 (trace)	nd[d] (nd)
10[e]	$[Cp^*RhCl_2]_2$	CsOAc	83 (83)	67 (63)	5:1 (5:1)
11	$[Cp^*RhCl_2]_2$	Mg/Al-CO_3^{2-}-LDHs	68	38	8:1
12	delaminated Ni/Al-Ala-Cp*Rh-LDHs		83	68	>20:1
13	delaminated Zn/Al-Ala-Cp*Rh-LDHs		62	57	18:1

[a]Reaction conditions: **1a** (0.150 mmol), **2a** (0.165 mmol), $[Cp^*RhCl_2]_2$ (0.500 mol %), ligand (α-amino acid anions 0.550 mol %), solvent (methanol 745 μL, H_2O 1750 μL). [b]Determined by ^{1}H NMR. [c]Isolated yield = 95%. [d]Not determined. [e]Using 0.500 mol % of $[Cp^*RhCl_2]_2$ with 2 equiv of CsOAc in 24 h. The figures in the parentheses are reproduced results.

dx.doi.org/10.1021/cs500558s | ACS Catal. 2014, 4, 3543−3550

avoided and the contact area is quite wide, no inhibition of catalytic activation occurring. Second, Mg/Al-LDH nanosheets, could not only serve as a strong solid base, but also promoted the C−H activation more efficiently than an exogenous strong solution base. The basicities of the α-amino acids-modified Mg/Al-LDHs were evaluated by the typical indicator titration method, according to the previous reports.[21] The Mg/Al-His-LDHs show basic sites with pK_a values up to 15.0, and the rest of the α-amino acids-modified Mg/Al-LDHs show basic sites with pK_a values in the 12.2−15.0 range, which are higher than the pK_a value of acetate ion (9.24),[24] indicating a stronger basicity of Mg/Al-LDHs than acetate ion. Even with simple Mg/Al-CO_3-LDHs, 68% conversion and 38% yield were produced (Table 1, entry 11). Higher yield has been achieved with only 0.5 mol % Rh, using Mg/Al-LDH nanosheets in this work, rather than using CsOAc in previous reports (95% yield with 2.5 mol % $[Cp^*RhCl_2]_2$[6a] and 95% yield with 1.0 mol % $[Cp^*RhCl_2]_2$[15]).

The dependence of conversion on the basicity of brucite-like layers[17b−e] further confirms the assistance of LDH nanosheet as a base. For Ni/Al-LDHs, with a lower basicity than Mg/Al-Ala-LDHs, 83% conversion was observed (Table 1, entry 12). For Zn/Al-Ala-LDHs, with a lower basicity than Ni/Al-Ala-LDHs, 62% conversion was observed (Table 1, entry 13).

The LDH nanosheets not only promote the conversion in Rh(III)-catalyzed C−H activation, but also cause the improvement of the regioisomeric ratio (rr), as can be clearly seen from Table 1. Modifying AA ligands with LDH nanosheets, >20:1 rr (**3aa** vs **4aa**) of dihydroisoquinolone was achieved (Table 1, entries 1−5), which is much higher than the rr of 5:1 without LDH nanosheets (Table 1, entry 10). Even with simple Mg/Al-CO_3-LDHs, 8:1 rr was produced (Table 1, entry 11). So the desired steric hindrance around Rh(III) center provided by LDH nanosheets to direct the access of attacking substrate can be deduced, just as expected. To elucidate the steric effects of LDH nanosheets, the orientations of interlayer AA anions have been tuned (Figure 3). A regioisomeric ratio (rr) of >20:1 has

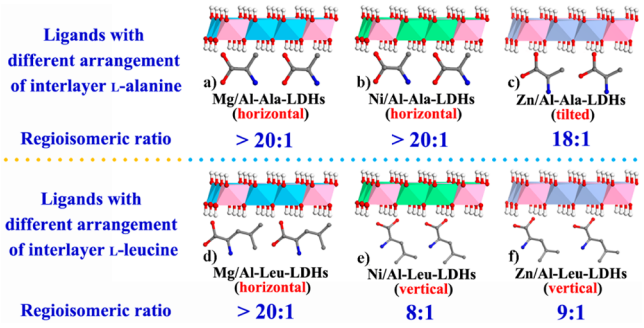

Figure 3. Dependence of regioisometric ratio on the orientation of interlayer AA anions: (a) Mg/Al-Ala-LDHs, (b) Ni/Al-Ala-LDHs, (c) Zn/Al-Ala-LDHs, (d) Mg/Al-Leu-LDHs, (e) Ni/Al-Leu-LDHs, and (f) Zn/Al-Leu-LDHs.

been achieved with the interlayer AA anions orientated in a horizontal arrangement (Figures 3a, 3b, and 3d). With the interlayer AA anions orientated in a tilted arrangement (Figure 3c), a value of 18:1 rr has been observed. Only 8:1 or 9:1 rr has been produced (Figures 3, 3e, and 3f) with the AA anions in a vertical arrangement. With the AA anions attached to the LDH brucite-like layers in a horizontal arrangement, the Cp* ligand is supposed to be positioned parallel to the LDH nanosheets, affording the desired steric hindrance around the Rh(III) center. The steric hindrance decreases with the interlayer AA orientation deviating from horizontal arrangement, causing the reduction of rr in the C−H activation reaction.

The substrate scope and generality of the designed Rh(III) catalysts with delaminated Mg/Al-Ala-LDHs as ligands was then explored (see Table 2). A yield of >99% and 19:1 rr of the

Table 2. Substrate Scope for Rh(III)-Catalyzed C−H Activation of *N*-(pivaloyloxy)benzamide and Alkenes[a]

entry	1	2	T (°C)	Time (h)	Yield[b] (%)	Regioisomeric ratio[b]
1	1a	 2b	25	10	> 99 (> 99)	19:1 (17:1)
2	1a	 2c	25	10	93 (92)	16:1 (17:1)
3	1a	 2d	25	10	25 (24)	18:1 (19:1)
4	1a	 2e	25	10	73 (78)	> 20:1 (> 20:1)
5	1a	 2f	25	10	54 (58)	> 20:1 (> 20:1)
6	1a	 2g	25	10	77 (81)	> 20:1 (> 20:1)
7	1a	 2h	25	10	75 (70)	> 20:1 (> 20:1)
8	1a	 2i	25	10	26 (32)	> 20:1 (> 20:1)
9[c]	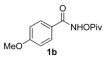 1b	2a	60	3	39 (45)	> 20:1 (> 20:1)
10[c]	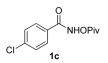 1c	2a	60	3	75 (69)	> 20:1 (> 20:1)
11[c]	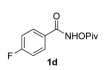 1d	2a	60	3	82 (76)	16:1 (15:1)
12[c]	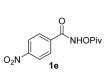 1e	2a	60	3	69 (71)	> 20:1 (> 20:1)

[a]Reaction conditions: **1a** (0.150 mmol), **2a** (0.165 mmol), $[Cp^*RhCl_2]_2$ (0.500 mol %), ligand (α-amino acid anions 0.550 mol %), solvent (methanol 745 μL, H_2O 1750 μL). [b]Determined by ^1H NMR. [c]The reaction was carried out at 60 °C because of the solubility of the *N*-(pivaloyloxy)benzamide derivatives. The figures in the parentheses are reproduced results.

desired product was produced in the C−H activation of *N*-(pivaloyloxy) benzamide (**1a**) with ethyl acrylate (**2b**) (Table 2, entry 1), 95% yield and 16:1 rr with *n*-butyl acrylate (**2c**) (Table 2, entry 2), and 25% yield and 18:1 rr with phenyl acrylate (**2d**) (Table 2, entry 3). The yield decreases as the steric hindrance of the substituent in acrylate derivatives increases. Then, the alkenes were extended from acrylates to styrene and 1-hexene. A yield of 73% and >20:1 rr of the desired product was produced with styrene (**2e**) (Table 2, entry 4), and 54% yield and >20:1 rr with 1-hexene (**2f**) (Table 2, entry 5). To examine the influence of electronic effect of alkenes on the outcomes, the reactions of **1a** with various substituted styrenes were then carried out. A yield of 77% and >20:1 rr of the desired product was produced with 4-methoxystyrene (**2g**) (Table 2, entry 6), 75% yield and >20:1 rr with 4-chlorostyrene (**2h**) (Table 2, entry 7), and 26% yield and >20:1 rr with 4-nitrostyrene (**2i**) (Table 2, entry 8). Electron-rich styrene is more favored than electron-deficient styrene. For *N*-(pivaloyloxy) benzamide derivatives, such

dx.doi.org/10.1021/cs500558s | ACS Catal. 2014, 4, 3543−3550

important functional groups as methoxy- (**1b**), chloro- (**1c**), fluoro- (**1d**), and nitro- (**1e**) substituents are all compatible in the Rh(III)-catalyzed C−H activation reaction with Mg/Al-Ala-LDHs as ligands. The desired products have been afforded in 39% yield and >20:1 rr for **1b** with methyl acrylate (**2a**) (Table 2, entry 9), 75% yield and >20:1 rr for **1c** (Table 2, entry 10), 82% yield and 16:1 rr for **1d** (entry 11), and 69% yield and >20:1 rr for **1e** (Table 2, entry 12). The substrates with electron-withdrawing substituents are more favored than the substrates with electron-donating substituents of hydroxamic acids, which is inconsistent with previous observation.[6a] Previous research on Rh(III) centers with acetate ions as ligands observed no change of the reaction outcome with the electron-withdrawing or electron-donating character of the substituents.[6a] This is proposed to originate from stronger electron-donating ability of LDH nanosheet-modified amino acid anions than acetate ions to the Rh center. As can be seen from the FT-IR spectra (Figure 4A), the asymmetric and

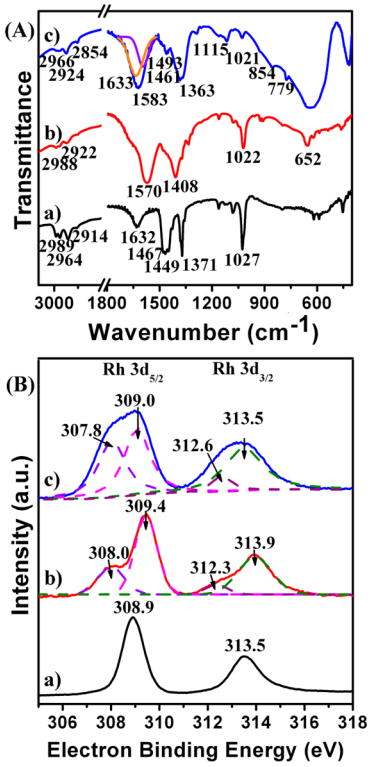

Figure 4. (A) FT-IR spectra and (B) XPS spectra of the $[Cp^*RhCl_2]_2$ precursor (spectrum a), $[Cp^*RhCl_2]_2$ with CsOAc introduced (spectrum b), and $[Cp^*RhCl_2]_2$ with Mg/Al-Ala-LDHs introduced (spectrum c).

symmetric vibrations of the carboxylate group are resolved at 1583 and 1363 cm^{-1} in the Mg/Al-Ala-Cp*Rh-LDH, indicating the interaction with $[Cp^*RhCl_2]_2$ has no obvious disruption on the carboxylate absorption of LDH nanosheet-modified L-alanine. However, the N−H out-of-plane vibration shifts from 746 cm^{-1} to 779 cm^{-1}, demonstrating the coordination of the amine-N of nanosheet-modified L-alanine to the Rh center. Meanwhile, the stretching vibrations of $-CH_3$ groups in the Cp* ligands (Cp* = pentamethylcyclopentadienyl)[25] shift from 2989, 2964, and 2914 cm^{-1} to 2966, 2924, and 2854 cm^{-1}. The rocking vibration of $-CH_3$ groups shift from 1027 to 1021 cm^{-1}. The blue shift of the N−H out-of-plane vibration and the red shift of the $-CH_3$ stretching vibrations verify the electron transfer from amine-N to the Rh complex. The change of electron density of Rh center is confirmed by the XPS analysis (Figure 4B) of $[Cp^*RhCl_2]_2$, $[Cp^*RhCl_2]_2$ with CsOAc introduced, and $[Cp^*RhCl_2]_2$ with Mg/Al-Ala-LDHs introduced. The XPS spectra of $[Cp^*RhCl_2]_2$ show the binding energy of Rh $3d_{5/2}$ and Rh $3d_{3/2}$ at 308.9 and 313.5 eV, respectively. The binding energy of Rh $3d_{5/2}$ of $[Cp^*RhCl_2]_2$ with CsOAc introduced splits into 308.0 and 309.4 eV, and Rh $3d_{3/2}$ splits into 312.3 and 313.9 eV. The binding energy of Rh $3d_{5/2}$ of $[Cp^*RhCl_2]_2$ with Mg/Al-Ala-LDHs introduced splits into 307.8 and 309.0 eV, and Rh $3d_{3/2}$ splits into 312.6 and 313.5 eV. The XPS results indicate that the rhodium centers are present in both Rh^{3+} and Rh^+ forms.[26] The existence of Rh^+ is supposed to result from the rapid equilibrium in the monodentate and bidentate coordination of ligands to Cp*Rh species.[27] The binding energy of Rh $3d_{5/2}$ of $[Cp^*RhCl_2]_2$ with Mg/Al-Ala-LDHs introduced is lower than that of $[Cp^*RhCl_2]_2$ with CsOAc introduced, suggesting a higher electron density for the Rh coordinated with the amine-N atom than with acetate-O atom. The amine-N coordination provides Rh center with high electron density, which might make it much more favorable for the Rh center to attach the hydroxamic acids with electron-withdrawing substituents.

The recycling experiment of the designed Rh(III) catalyst with delaminated Mg/Al-Ala-LDHs as ligands has been carried out. The yield decreased from >99% to 63% in the second run and 19% in the third run within 12 h, while the regioisomeric ratio fully retained at >20:1. Fifteen milligrams (15 mg) of Mg/Al-CO_3^--LDHs was added to the reaction system after the third run. Within 24 h, a yield of 86% was afforded in the fourth run and 74% in the fifth run. The −OH groups of the delaminated LDH layers might be consumed in the reaction, but the catalyst recycling could be achieved through adding LDHs solid. To understand the reason for low reusability of the Rh(III) catalyst in the recycling experiments, the rhodium leaching has been monitored. The rhodium loss in solution was 3.2%, 2.4%, 2.0%, 1.4%, and 1.1% in each catalytic run. The rhodium loss is not enough to cause a large decline of the yield in the catalytic run. Thus, the rhodium loss is not the main reason for the low reusability of the Rh(III) catalyst. Then, the structure of the recovered Rh(III) catalyst with Mg/Al-CO_3^{2-}-LDH nanosheets as the base has been investigated by examining the XRD pattern and FT-IR spectrum (Figure 5). The XRD pattern of the recovered Rh(III) catalyst with Mg/Al-CO_3^{2-}-LDH nanosheets as the base preserves the reflections of the fresh Mg/Al-CO_3^{2-}-LDH nanosheets, except the appearance of two new reflections at 2θ = 8.26° and 9.53°. In the FT-IR spectrum of the recovered Rh(III) catalyst with Mg/Al-CO_3^{2-}-LDH nanosheets as the base, the appearance of the absorptions assigned to stretching vibrations of $-CH_3$ groups at 2965, 2930, and 2871 cm^{-1}, the sharp absorption assigned to the asymmetric vibration of −COOH group at 1587 cm^{-1}, and the two absorptions assigned to typical bending vibrations of *tert*-butyl group at 1492 and 1446 cm^{-1} indicates that pivalic acid, a co-product in the C−H activation reaction of *N*-(pivaloyloxy)benzamide with methyl acrylate, has been adsorbed on the LDH nanosheets. In combination with the XRD pattern, the intercalation of pivalic acid could not be excluded. The pivalic acid adsorption could be the main reason for the yield decrease in the recycling experiments.

dx.doi.org/10.1021/cs500558s | ACS Catal. 2014, 4, 3543−3550

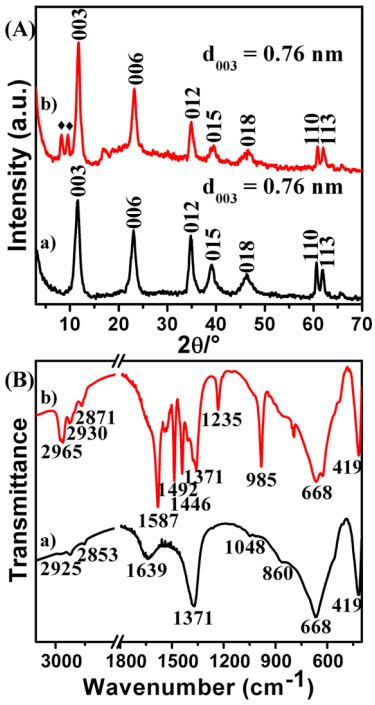

Figure 5. (A) XRD patterns and (B) FT-IR spectra of fresh Mg/Al-CO_3^{2-}-LDH nanosheets (spectrum a) and recovered Rh(III) catalyst with Mg/Al-CO_3^{2-}-LDH nanosheets as the base (spectrum b).

CONCLUSIONS

In summary, this work has demonstrated the highly efficient rhodium(III)-catalyzed C−H activations achieved by using LDH nanosheets-modified-AA anions as ligands. Yields of >99% and a regioisomeric ratio of >20:1 of final products were afforded. The nanosheets were revealed to enhance the catalytic activity by affording the desired basicity, and improve the regioselectivity by serving as the rigid substitution of AA ligands. The application of the rhodium catalysts with LDH nanosheets-modified-AA anions as ligands in more C−H bond activations is currently underway.

ASSOCIATED CONTENT

Supporting Information

^{1}H NMR, ^{13}C NMR, IR, and HRMS analysis for catalyzed substrates and products. This material is available free of charge via the Internet at http://pubs.acs.org/.

AUTHOR INFORMATION

Corresponding Author

*Tel.: +86-10-64425280. Fax: +86-10-64425385. E-mail: hejing@mail.buct.edu.cn.

Notes

The authors declare no competing financial interest.

ACKNOWLEDGMENTS

This work is supported by NSFC, PCSIRT (IRT1205), 973 Project (No. 2011CBA00504), and the Fundamental Research Funds for the Central Universities. J.H. particularly appreciates the financial aid of China National Funds for Distinguished Young Scientists from the NSFC.

REFERENCES

(1) (a) Matsumoto, T.; Yoshida, H. *Chem. Lett.* **2000**, 1064−1065. (b) Matsumoto, T.; Periana, R. A.; Taube, D. J.; Yoshida, H. *J. Catal.* **2002**, *206*, 272−280.

(2) For selected reviews regarding rhodium catalyzed C-H activation, see: (a) Kuhl, N.; Schröder, N.; Glorius, F. *Adv. Synth. Catal.* **2014**, *356*, 1443−1460. (b) Patureau, F. W.; Wencel-Delord, J.; Glorius, F. *Aldrichimica Acta* **2012**, *45*, 31−41. (c) Song, G.; Wang, F.; Li, X. W. *Chem. Soc. Rev.* **2012**, *41*, 3651−3678. (d) Satoh, T.; Miura, M. *Chem.—Eur. J.* **2010**, *16*, 11212−11222.

(3) (a) Tauchert, M. E.; Incarvito, C. D.; Rheingold, A. L.; Bergman, R. G.; Ellman, J. A. *J. Am. Chem. Soc.* **2012**, *134*, 1482−1485. (b) Hesp, K. D.; Bergman, R. G.; Ellman, J. A. *J. Am. Chem. Soc.* **2011**, *133*, 11430−11433. (c) Tsai, A. S.; Tauchert, M. E.; Bergman, R. G.; Ellman, J. A. *J. Am. Chem. Soc.* **2011**, *133*, 1248−1250.

(4) Wang, C.; Chen, H.; Wang, Z.; Chen, J.; Huang, Y. *Angew. Chem., Int. Ed.* **2012**, *51*, 7242−7245.

(5) (a) Shi, Z.; Grohmann, C.; Glorius, F. *Angew. Chem., Int. Ed.* **2013**, *52*, 5393−5397. (b) Schröder, N.; Wencel-Delord, J.; Glorius, F. *J. Am. Chem. Soc.* **2012**, *134*, 8298−8301. (c) Grohmann, C.; Wang, H.; Glorius, F. *Org. Lett.* **2012**, *14*, 656−659. (d) Patureau, F. W.; Besset, T.; Kuhl, N.; Glorius, F. *J. Am. Chem. Soc.* **2011**, *133*, 2154−2156. (e) Patureau, F. W.; Besset, T.; Glorius, F. *Angew. Chem., Int. Ed.* **2011**, *50*, 1064−1067. (f) Rakshit, S.; Grohmann, C.; Besset, T.; Glorius, F. *J. Am. Chem. Soc.* **2011**, *133*, 2350−2353. (g) Patureau, F. W.; Glorius, F. *J. Am. Chem. Soc.* **2010**, *132*, 9982−9983. (h) Rakshit, S.; Patureau, F. W.; Glorius, F. *J. Am. Chem. Soc.* **2010**, *132*, 9585−9587.

(6) (a) Guimond, N.; Gorelsky, S. I.; Fagnou, K. *J. Am. Chem. Soc.* **2011**, *133*, 6449−6457. (b) Huestis, M. P.; Chan, L.; Stuart, D. R.; Fagnou, K. *Angew. Chem., Int. Ed.* **2011**, *50*, 1338−1341. (c) Guimond, N.; Gouliaras, C.; Fagnou, K. *J. Am. Chem. Soc.* **2010**, *132*, 6908−6909. (d) Guimond, N.; Fagnou, K. *J. Am. Chem. Soc.* **2009**, *131*, 12050−12051. (e) Stuart, D. R.; Bertrand-Laperle, M.; Burgess, K. M. N.; Fagnou, K. *J. Am. Chem. Soc.* **2008**, *130*, 16474−16475.

(7) Hyster, T. K.; Rovis, T. *J. Am. Chem. Soc.* **2010**, *132*, 10565−10569.

(8) Umeda, N.; Tsurugi, H.; Satoh, T.; Miura, M. *Angew. Chem., Int. Ed.* **2008**, *47*, 4019−4022.

(9) (a) Zhang, Q.; Yu, H. Z.; Li, Y. T.; Liu, L.; Huang, Y.; Fu, Y. *Dalton Trans.* **2013**, *42*, 4175−4184. (b) Xu, L.; Zhu, Q.; Huang, G.; Cheng, B.; Xia, Y. *J. Org. Chem.* **2012**, *77*, 3017−3024.

(10) (a) Ng, K. H.; Zhou, Z.; Yu, W. Y. *Org. Lett.* **2012**, *14*, 272−275. (b) Zhang, X.; Chen, D.; Zhao, M.; Zhao, J.; Jia, A.; Li, X. *Adv. Synth. Catal.* **2011**, *353*, 719−723.

(11) Too, P. C.; Wang, Y. F.; Chiba, S. *Org. Lett.* **2010**, *12*, 5688−5691.

(12) Too, P. C.; Chua, S. H.; Wong, S. H.; Chiba, S. *J. Org. Chem.* **2011**, *76*, 6159−6168.

(13) Ackermann, L. *Chem. Rev.* **2011**, *111*, 1315−1345.

(14) Ackermann, L. *Acc. Chem. Res.* **2014**, *47*, 281−295.

(15) Hyster, T. K.; Knörr, L.; Ward, T. R.; Rovis, T. *Science* **2012**, *338*, 500−503.

(16) (a) Paradowska, J.; Stodulski, M.; Mlynarski, J. *Angew. Chem., Int. Ed.* **2009**, *48*, 4288−4297. (b) Severin, K.; Bergs, R.; Beck, W. *Angew. Chem., Int. Ed.* **1998**, *37*, 1634−1654.

(17) (a) He, S.; An, Z.; Wei, M.; Evans, D. G.; Duan, X. *Chem. Commun.* **2013**, *49*, 5912−5920. For selected examples regarding LDHs as base catalysts, see: (b) Manivannan, R.; Pandurangan, A. *Appl. Clay Sci.* **2009**, *44*, 137−143. (c) Khan, F. A.; Dash, J.; Satapathy, R.; Upadhyay, S. K. *Tetrahedron Lett.* **2004**, *45*, 3055−3058. (d) Costantino, U.; Curini, M.; Montanari, F.; Nocchetti, M.; Rosati, O. *J. Mol. Catal. A: Chem.* **2003**, *195*, 245−252. (e) Honma, T.; Nakajo, M.; Mizugaki, T.; Ebitani, K.; Kaneda, K. *Tetrahedron Lett.* **2002**, *43*, 6229−6232. (f) Yamaguchi, K.; Mori, K.; Mizugaki, T.; Ebitani, K.; Kaneda, K. *J. Org. Chem.* **2000**, *65*, 6897−6903. (g) Dumitriu, E.; Hulea, V.; Chelaru, C.; Catrinescu, C.; Tichit, D.; Durand, R. *Appl. Catal., A* **1999**, *178*, 145−157. (h) Choudary, B. M.; Lakshmi Kantam, M.; Kavita, B.; Venkat Reddy, C.; Koteswara Rao,

K.; Figueras, F. *Tetrahedron Lett.* **1998**, *39*, 3555−3558. (i) Lakshmi Kantam, M.; Choudary, B. M.; Venkat Reddy, C.; Koteswara Rao, K.; Figueras, F. *Chem. Commun.* **1998**, 1033−1034.
(18) (a) Whilton, N. T.; Vickers, P. J.; Mann, S. *J. Mater. Chem.* **1997**, *7*, 1623−1629. (b) Aisawa, S.; Takahashi, S.; Ogasawara, W.; Umetsu, Y.; Narita, E. *J. Solid State Chem.* **2001**, *162*, 52−62.
(19) Nakayama, H.; Wada, N.; Tsuhako, M. *Int. J. Pharm.* **2004**, *269*, 469−478.
(20) (a) Jaubertie, C.; Holgado, M. L.; San Román, M. S.; Rives, V. *Chem. Mater.* **2006**, *18*, 3114−3121. (b) Hibino, T.; Kobayashi, M. *J. Mater. Chem.* **2005**, *15*, 653−656.
(21) (a) Ueno, S.; Ebitani, K.; Ookubo, A.; Kaneda, K. *Appl. Surf. Sci.* **1997**, *121/122*, 366−371. (b) Take, J. I.; Kikuchi, N.; Yoneda, Y. *J. Catal.* **1971**, *21*, 164−170. (c) Kagunya, W.; Hassan, Z.; Jones, W. *Inorg. Chem.* **1996**, *35*, 5970−5974.
(22) (a) Prevot, V.; Forano, C.; Besse, J. P. *Inorg. Chem.* **1998**, *37*, 4293−4301. (b) Kakihana, M.; Nagumo, T. *J. Phys. Chem.* **1987**, *91*, 6128−6137.
(23) Wang, J. Z.; Zhao, L. W.; Shi, H. M.; He, J. *Angew. Chem., Int. Ed.* **2011**, *50*, 9171−9176.
(24) *Lange's Handbook of Chemistry*, 16th Edition; Speight, J. G., Ed.; McGraw−Hill: New York, 2005; Table 1.66.
(25) Abbasi, A.; Geranmayeh, S.; Skripkin, M. Y.; Eriksson, L. *Dalton Trans.* **2012**, *41*, 850−859.
(26) Wang, L.; Sowa, J. R.; Wang, C.; Lu, R. S.; Gassman, P. G.; Flood, T. C. *Organometallics* **1996**, *15*, 4240−4246.
(27) Li, L.; Brennessel, W. W.; Jones, W. D. *Organometallics* **2009**, *28*, 3492−3500.